

Diffeomorphic Point Matching

H. Guo, A. Rangarajan, S. C. Joshi

ABSTRACT In medical imaging and computer vision, the problem of registering point-sets that differ by an unknown non-rigid transformation frequently arises. We discuss the matching problem of shapes parameterized by point sets. Mathematical models of diffeomorphic landmark matching and diffeomorphic point shape matching are formulated. After formulating an objective function for diffeomorphic point matching, we give numerical algorithms to solve the objective. Results are shown for 2D corpus callosum shapes.

Keywords: image registration, non-rigid, diffeomorphism, point matching, biomedical imaging, topology, landmark, cluster, thin-plate spline, interpolation, correspondence, EM algorithm

1 Introduction

Point matching and correspondence problems arise in various application areas such as computer vision, pattern recognition, machine learning and especially in computational anatomy and biomedical imaging. Point representation of image data is widely used in all areas and there is a huge amount of point feature data acquired in various modalities, including MRI, CT and Diffusion Tensor Images (DTI) [7, 10, 6]. The advantage of point set representations of shapes over other forms like curves and surfaces is that the point set representation is a universal representation of shapes regardless of the topologies of the shapes. This is especially useful in biomedical imaging because it has the ability to fuse different types of anatomical features in a single uniform representation.

Point matching in general is a difficult problem because, as with many other problems in computer vision, like image registration and segmentation, it is often ill-posed. In this chapter, we attempt to formulate a precise mathematical model for point matching. There are two important cases that need to be distinguished. When the two point-sets are of equal cardinality and when the correspondences are known, we have the *landmark matching problem*. This problem is not as difficult as the case when the correspondences are unknown. When we have two point-sets of unequal cardinality and when the correspondences are unknown, we have the *point shape matching problem*. The presence of outliers in either/both sets makes the correspondence problem even more difficult. In the following, we will

first discuss the landmark matching problem and then the point shape matching problem.

2 Diffeomorphic Landmark Matching

We assume the image domain is the d -dimensional Euclidean space \mathbf{R}^d . Usually $d = 2$ or $d = 3$. In landmark based registration, we assume that we have two corresponding sets of feature points, or landmarks, $\{p_i \in \Omega_1 | i = 1, 2, \dots, n\}$ and $\{q_i \in \Omega_2 | i = 1, 2, \dots, n\}$ where $\Omega_1 \subseteq \mathbf{R}^d$ and $\Omega_2 \subseteq \mathbf{R}^d$. We need to find a transformation $f : \Omega_1 \rightarrow \Omega_2$ such that $\forall i = 1, 2, \dots, n$, $f(p_i) = q_i$.

In many applications, we are required to find the transformation within some restricted groups, like rigid transformations, similarity transformations, affine transformations, projective transformations, polynomial transformations, B-spline transformations and “non-rigid” transformations. Different transformation groups have different degrees of freedom, namely, the number of parameters needed to describe a transformation in the group. This also determines the number of landmark pairs that the transformation can exactly interpolate. Let us look at some examples. In two dimensional space, where $d = 2$, a rigid transformation, which preserves Euclidean distance, has 3 degrees of freedom and cannot interpolate arbitrary landmark pairs. The landmark pairs to be matched must be subject to some constraints. That is, they have to have the same Euclidean distance. A similarity transformation has 4 degrees of freedom and can map any 2 points to any 2 points. An affine transformation has 6 degrees of freedom and can map any 3 non-degenerate points to any 3 non-degenerate points. A projective transformation has 8 degrees of freedom and can map any 4 non-degenerate points to any 4 non-degenerate points. In three dimensional space, where $d = 3$, a rigid transformation has 6 degrees of freedom. A similarity transformation has 7 degrees of freedom. An affine transformation has 12 degrees of freedom and can map any 4 non-degenerate points to any 4 non-degenerate points. A projective transformation has 15 degrees of freedom and can map any 5 non-degenerate points to any 5 non-degenerate points.

The term “non-rigid” transformation is often used in a narrower sense. Although similarity, affine and projective transformations do not preserve Euclidean distance, they all have finite degrees of freedom. In the literature, “non-rigid” transformations usually refer to a transformation with infinite degrees of freedom, which can potentially map any finite number of points to the same number of points. So we immediately see a big difference between finite degree of freedom transformations and non-rigid transformations. Given a fixed number of landmark pairs to be interpolated, the former is easily over constrained but the latter is always under constrained. This is

one of the reasons why the non-rigid point matching problem is much more difficult. To find a unique non-rigid transformation, we need further constraints. This is termed regularization in the computer vision and medical image analysis literature [11].

Two desirable properties of non-rigid transformations are smoothness and topology preservation. Again, let $\Omega_1 \subseteq \mathbf{R}^d$ and $\Omega_2 \subseteq \mathbf{R}^d$. A transformation $f : \Omega_1 \rightarrow \Omega_2$ is said to be smooth if all partial derivatives of f , up to certain orders, exist and are continuous. A transformation $f : \Omega_1 \rightarrow \Omega_2$ is said to preserve the topology if Ω_1 and $\text{Img}(f) = \{p_2 \in \Omega_2 | \exists p_1 \in \Omega_1, p_2 = f(p_1)\}$ have the same topology. A transformation that preserves topology is called a *homeomorphism* and its definition is: A transformation $f : \Omega_1 \rightarrow \Omega_2$ is a homeomorphism if f is a bijection and if it is continuous and if its inverse is also continuous. A smooth transformation $f : \Omega_1 \rightarrow \Omega_2$ may not preserve the topology. There are several cases when this is true. First, the smooth map f is a bijection but the inverse is not continuous. Second, the smooth map f may fail to be a bijection. That is, multiple points may be mapped to the same point and we call this the folding of space. There are two sub-cases here, one sub-case is that at some point, the tangent map of f is not an isomorphism. The other sub-case is that the tangent map of f is an isomorphism at every point but globally it is not a bijection. On the other hand, a homeomorphism may not be smooth because in the definition, we only require continuity in both f and its inverse but we do not require differentiability. A transformation f that is both smooth and topology preserving is called a *diffeomorphism*. The diffeomorphism $f : \Omega_1 \rightarrow \Omega_2$ is defined as a bijection that is smooth and its inverse is also smooth. Now let us look at an example of a smooth transformation, namely, the Thin-Plate Spline (TPS) interpolation [17].

For simplicity, we discuss the problem in 2-D space. Everything in the 2-D formulation easily applies to 3-D except we have a different kernel in 3-D. The original thin-plate spline interpolation problem is formulated as: find a smooth function $f : \Omega \rightarrow \mathbf{R}$, such that the thin-plate energy $\int \int_{\Omega} \left[\left(\frac{\partial^2 f}{\partial x^2} \right)^2 + 2 \left(\frac{\partial^2 f}{\partial x \partial y} \right)^2 + \left(\frac{\partial^2 f}{\partial y^2} \right)^2 \right] dx dy$ is minimized, subject to constraints at n control points $\{p_i \in \Omega | i = 1, 2, \dots, n\}$

$$f(p_i) = v_i, p_i \in \Omega, v_i \in \mathbf{R}, i = 1, 2, \dots, n. \quad (1.1)$$

The reproducing kernel Hilbert space (RKHS) method is used to solve this problem. We assume f is in the Sobolev space $W^{k,2}(\Omega)$. Let $\|f\|^2 = E = \int \int_{\Omega} \left[\left(\frac{\partial^2 f}{\partial x^2} \right)^2 + 2 \left(\frac{\partial^2 f}{\partial x \partial y} \right)^2 + \left(\frac{\partial^2 f}{\partial y^2} \right)^2 \right] dx dy$, where $\|f\|$ is the norm of f in $W^{k,2}(\Omega)$. Since $W^{k,2}(\Omega)$ is a Hilbert space, from the Riesz representation theorem, for any $p \in \Omega$, the evaluation linear functional

$$\delta_p : W^{k,2}(\Omega) \rightarrow \mathbf{R}, \delta_p(f) = f(p) \quad (1.2)$$

has a representer [15] $u_p \in W^{k,2}(\Omega)$ such that

$$\delta_p(f) = f(p) = \langle u_p, f \rangle. \quad (1.3)$$

Now the original problem is transformed to the problem: find a function $f \in W^{k,2}(\Omega)$ with minimal norm $\|f\|$, subject to constraints

$$\langle u_{p_i}, f \rangle = v_i, \quad i = 1, 2, \dots, n. \quad (1.4)$$

For $p_a, p_b \in \Omega$, $u(p_a, p_b) = u_{p_a}(p_b)$ is the kernel of the reproducing kernel Hilbert space.

Let T be the linear subspace spanned by u_{p_i} , $i = 1, 2, \dots, n$. Any function $f \in W^{k,2}(\Omega)$ can be decomposed into $f = f_T + f_\perp$ where $f_T \in T$ and f_\perp is in the orthogonal complement of T and hence $\langle u_{p_i}, f_\perp \rangle = 0$. We know if f_T satisfies (1.4), then f also satisfies (1.4) only with $\|f\| > \|f_T\|$ if $f_\perp \neq 0$. So we only need to search for the solution in T . The general solution can thus be written as

$$f(p) = a_0 + a_1x + a_2y + \sum_{i=1}^n w_i u(p_i, p), \quad (1.5)$$

where $a_0, a_1, a_2, w_i \in \mathbf{R}$ and functions of the form $a_0 + a_1x + a_2y$ span the null space.

With this form, E can be rewritten as

$$E = \sum_{i=1, j=1}^n w_i U_{ij} w_j = W U W^+, \quad (1.6)$$

where $W = (w_1, \dots, w_n)$ and U is the matrix with elements $U_{ij} = u(p_i, p_j)$.

Bookstein [1, 2] applied thin-plate splines to the landmark interpolation problem. The goal is to find a smooth transformation $f : \Omega \rightarrow \Omega$ that interpolates n pairs of landmarks $\{p_i \in \Omega \mid i = 1, 2, \dots, n\}$ and $\{q_i \in \Omega \mid i = 1, 2, \dots, n\}$ and also minimize the thin-plate bending energy

$$E = \sum_{h=1}^2 \int \int_{\mathbf{R}^2} \left[\left(\frac{\partial^2 f_h}{\partial x^2} \right)^2 + 2 \left(\frac{\partial^2 f_h}{\partial x \partial y} \right)^2 + \left(\frac{\partial^2 f_h}{\partial y^2} \right)^2 \right] dx dy, \quad (1.7)$$

where f_1 and f_2 are the x and y components of the mapping. If we interpret each of f_1 and f_2 as the bending in the z direction of a metal sheet, or thin plate, extending in the x - y plane, the energy in (1.7) is the analog of the thin plate bending energy. The kernel in this case is

$$U(r) = r^2 \log r^2, \quad (1.8)$$

where r is the distance $\sqrt{x^2 + y^2}$. We also denote

$$P = \begin{bmatrix} 1 & x_1 & y_1 \\ 1 & x_2 & y_2 \\ \dots & \dots & \dots \\ 1 & x_n & y_n \end{bmatrix}, \text{ which is } 3 \times n, \quad (1.9)$$

Duchon [8] proved that if P has maximum column rank, then the solution exists and is unique and the general solution is of the form

$$f(x, y) = a_1 + a_x x + a_y y + \sum_{i=1}^n w_i U(|p_i - (x, y)|). \quad (1.10)$$

Because an affine transformation has no contribution to the bending energy, the transformation allows for a free affine transformation. Define the matrices

$$K = \begin{bmatrix} 0 & U(r_{12}) & \dots & U(r_{1n}) \\ U(r_{21}) & 0 & \dots & U(r_{2n}) \\ \dots & \dots & \dots & \dots \\ U(r_{n1}) & U(r_{n2}) & \dots & 0 \end{bmatrix}, \text{ which is } n \times n, \quad (1.11)$$

and

$$L = \begin{bmatrix} K & P \\ P^T & O \end{bmatrix}, \text{ which is } (n+3) \times (n+3), \quad (1.12)$$

where the symbol T is the matrix transpose operator and O is a 3×3 matrix of zeros.

Let $V = (v_1, \dots, v_n)$ be any n -vector and write $Y = (V | 000)^T$. The coefficients $W = (w_1, \dots, w_n)$ and (a_1, a_x, a_y) can be found by

$$L^{-1}Y = (W | a_1 \ a_x \ a_y)^T. \quad (1.13)$$

A numerically stable solution in a different form is given by Wahba [17] using a QR decomposition.

While the preceding development is somewhat appealing, there is no mechanism to guarantee a diffeomorphic transformation. Intuitively this problem is known as the folding of space.

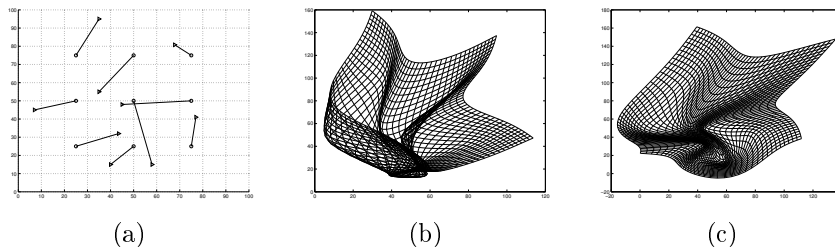


FIGURE 1. The folding problem in TPS and the desirable diffeomorphism.

Figure 1a shows the displacement of landmarks. Figure 1b is the thin-plate spline interpolation. We can see the folding of space. This is the drawback of thin-plate spline interpolation. Due to the folding of space, features in the template may be smeared in the overlapping regions. And furthermore, the transformation is not invertible. A diffeomorphic transformation is strongly desirable, which preserves the features, the topology and which is smooth as shown in Figure 1c. Next we show that such a diffeomorphism always exists.

Theorem. *A diffeomorphic transformation that interpolates arbitrary numbers of n pairs of landmarks always exists.*

Proof. We show the existence by construction. We construct a simple, although most likely undesirable in most of the applications, diffeomorphism. The intuitive idea is to dig canals connecting the landmark pairs. We first choose the first pair of landmarks p_1 and q_1 . For simplicity, we assume the dimension d of space is 2. The proof is similar for $d > 2$. First assume no other landmarks lie on the line connecting p_1 and q_1 . Establish a coordinate system such that p_1 and q_1 are on the x axis, shown in Figure 2, where dots are source landmarks and squares are target landmarks. Let the signed distance from p_1 to q_1 be a . Construct the transformation $f_1 : \Omega_1 \rightarrow \Omega_2$ such that $f_1(x, y) = (x', y')$,

$$\begin{aligned} x' &= x + ae^{-v^2} \\ y' &= y \end{aligned} \tag{1.14}$$

where $v = \tan(\frac{\pi}{2\epsilon}y)$, for any arbitrarily small ϵ . We choose ϵ to be sufficiently small so that any other landmarks do not lie in the belt $\{(x, y) \in \mathbf{R}^2 \mid |y| < \epsilon\}$.

It is easy to show that f_1 is a diffeomorphism and that it maps p_1 to q_1 and keeps all other landmarks q_2, \dots, q_n fixed. This is very much like the flow of viscous fluid in a tube. Similarly we can construct a diffeomorphism f_i that maps p_i to q_i and keeps all other landmarks fixed, for $i = 1, 2, \dots, n$. The composition of this series of diffeomorphisms

$$f = f_n \circ \dots \circ f_2 \circ f_1 \tag{1.15}$$

is also a diffeomorphism and obviously f maps p_i to q_i , for $i = 1, 2, \dots, n$.

If some landmark q_k lies on the line joining p_i and q_i , we can find such a direction such that we draw a line l_k through q_k and there are no other landmarks on the line. Then we make a diffeomorphism h transporting q_k to a nearby point q'_k along the line without moving any other landmarks, using the same canal as in the viscous fluid technique. Then we make a diffeomorphism f_i as described before. After that, we move landmark q'_k back to the old position with the inverse of h^{-1} . So we use $F_i = h^{-1}f_i h$ in place of f_i .

□

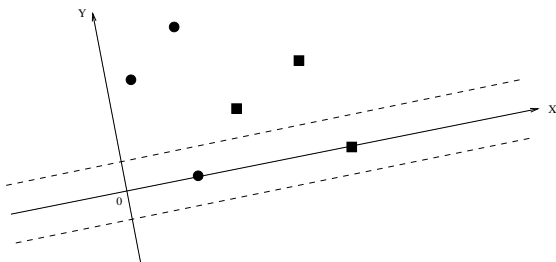


FIGURE 2. Diffeomorphism construction.

One straightforward approach to find a diffeomorphism for practical use is to remedy the thin-plate spline so that it does not fold. We can restrict our search space to the set of diffeomorphisms and the ideal one should minimize the thin-plate energy. We make the observation that if the Jacobian of the transformation f changes sign at a point, then there is folding. We can place a constraint requiring the Jacobian to always be positive. There is some literature on this approach but most of these approaches do not guarantee that the transformation is smooth [13, 4].

Another approach is to utilize the flow field [9, 14, 16]. We introduce one parameter, the time t into the diffeomorphism. Let $\phi_t : \Omega \rightarrow \Omega$ be the diffeomorphism from Ω to Ω at time t . A point x is mapped to the point $\phi_t(x)$. Sometimes we also denote this as $\phi(x, t)$. It is easy to verify that for all the values of t , ϕ_t forms a one parameter diffeomorphism group. If x is fixed, then $\phi(x, t)$ traces a smooth trajectory in Ω . The interpolation problem becomes: find the one parameter diffeomorphic group $\phi(\cdot, t) : \Omega \rightarrow \Omega$ such that given $p_i \in \Omega$ and $q_i \in \Omega \forall i = 1, 2, \dots, n$, $\phi(x, 0) = x$ and $\phi(p_i, 1) = q_i$. We introduce the velocity field $v(x, t)$ and construct a dynamical system by the transport equation

$$\frac{d\phi(x, t)}{dt} = v(\phi(x, t), t). \quad (1.16)$$

The integral form of the relation between $\phi(x, t)$ and $v(x, t)$ is

$$\phi(x, 1) = x + \int_0^1 v(\phi(x, t), t) dt. \quad (1.17)$$

Obviously, such a $\phi(x, t)$ is not unique and there are infinitely many such solutions. With the analogy to the TPS, it is natural that we require the desirable diffeomorphism results in minimal space deformation. Namely we require the deformation energy

$$\int_0^1 \int_{\Omega} \|Lv(x, t)\|^2 dx dt \quad (1.18)$$

to be minimized, where L is a given linear differential operator.

The following theorem [14] states the existence of such a velocity field and shows a way to solve for it.

Theorem (Joshi and Miller). *Let $p_i \in \Omega$ and $q_i \in \Omega \forall i = 1, 2, \dots, n$. The solution to the energy minimization problem*

$$\hat{v}(\cdot) = \arg \min \int_0^1 \int_{\Omega} \|Lv(x, t)\|^2 dx dt \quad (1.19)$$

subject to

$$\phi(p_i, 1) = q_i, \quad \forall i = 1, 2, \dots, n \quad (1.20)$$

where

$$\phi(x, 1) = x + \int_0^1 v(\phi(x, t), t) dt \quad (1.21)$$

exists and defines a diffeomorphism $\phi(\cdot, 1) : \Omega \rightarrow \Omega$. The optimum velocity field \hat{v} and the diffeomorphism $\hat{\phi}$ are given by

$$\hat{v}(x, t) = \sum_{i=1}^n K(\phi(x_i, t), x) \sum_{j=1}^n (K(\phi(t))^{-1})_{ij} \dot{\hat{\phi}}(x_j, t) \quad (1.22)$$

where

$$K(\phi(t)) = \begin{pmatrix} K(\phi(p_1, t), \phi(p_1, t)) & \cdot & \cdot & \cdot & K(\phi(p_1, t), \phi(p_n, t)) \\ \cdot & \cdot & \cdot & \cdot & \cdot \\ \cdot & \cdot & \cdot & \cdot & \cdot \\ \cdot & \cdot & \cdot & \cdot & \cdot \\ K(\phi(p_n, t), \phi(p_1, t)) & & & & K(\phi(p_n, t), \phi(p_n, t)) \end{pmatrix} \quad (1.23)$$

with $(K(\phi(t)))_{ij}$ denoting the ij , 3×3 block entry $(K(\phi(t)))_{ij} = K(\phi(p_i, t), \phi(p_j, t))$, and

$$\hat{\phi}(p_n, \cdot) = \arg \min_{\phi(p_n, \cdot)} \int_0^1 \sum_{ij} \phi(p_i, t)^T (K(\phi(t))^{-1})_{ij} \dot{\phi}(p_j, t) dt \quad (1.24)$$

subject to $\phi(p_i, 1) = q_i$, $i = 1, 2, \dots, N$ with the optimal diffeomorphism given by

$$\hat{\phi}(x, 1) = x + \int_0^1 \hat{v}(\phi(x, \hat{t}), t) dt. \quad (1.25)$$

The proof [14] is omitted here. With this theorem, we can convert the original optimization problem on the vector field $\hat{v}(x, t)$ to a problem of finite dimensional optimal control with end point conditions.

This problem is called the *exact matching problem* because we required the given set of points $p_i, i = 1, 2, \dots, n$ map exactly to the other given set of points $q_i, i = 1, 2, \dots, n$. The exact matching problem is symmetric with respect to two sets of landmarks or two point shapes. When the two point sets $\{p_i \in \Omega_1 | i = 1, 2, \dots, n\}$ and $\{q_i \in \Omega_2 | i = 1, 2, \dots, n\}$ are swapped, the new optimal diffeomorphism is the inverse of the old diffeomorphism. This is stated more formally in the following theorem.

Theorem. *If $\phi(x_k, 1) = y_k$ and $\phi(x, t)$ and $v(x, t)$ minimize the energy $E = \int_0^1 \int_{\Omega} \|Lv(x, t)\|^2 dx dt$, then the inverse mapping maps the landmarks backward $\phi^{-1}(y_k, 1) = x_k$ and $\phi^{-1}(x, t)$ and $-v(x, -t)$ also minimize the energy E .*

Proof. First, from the known property of the diffeomorphism group of such a dynamical system, $\phi(x, t_1 + t_2) = \phi(\phi(x, t_1), t_2)$, it is easy to show that $\phi^{-1}(x, t) = \phi(x, -t)$. This is because

$$\begin{aligned} & \phi(\cdot, -t) \circ \phi(\cdot, t)(x) \\ &= \phi(\cdot, t) \circ \phi(\cdot, -t)(x) \\ &= \phi(\phi(x, t), -t) \\ &= \phi(x, t + (-t)) \\ &= \phi(x, 0) \\ &= x. \end{aligned}$$

Furthermore, $\phi(x, -t)$ and $-v(x, -t)$ also satisfy the transport equation $\frac{d\phi(x, -t)}{dt} = -v(\phi(x, -t), -t)$. Suppose $\phi(x, t)$ and $v(x, t)$ minimize the energy $E = \int_0^1 \int_{\Omega} \|Lv(x, t)\|^2 dx dt$, but $\phi^{-1}(x, t) = \phi(x, -t)$ and $-v(x, -t)$ do not minimize the energy $E = \int_0^1 \int_{\Omega} \|Lv(x, t)\|^2 dx dt$. Let the minimizer be $\psi(x, t)$ and $u(x, t)$ such that $\forall k, \psi(y_k) = x_k$ and $\int_0^1 \int_{\Omega} \|Lu(x, t)\|^2 dx dt < \int_0^1 \int_{\Omega} \|Lv(x, t)\|^2 dx dt$. Then, we can construct $\psi^{-1}(x, t) = \psi(x, -t)$ such that $\psi^{-1}(x, t)$ and $-u(x, -t)$ satisfy the transport equation and $\psi^{-1}(x_k, 1) = y_k$. However $\int_0^1 \int_{\Omega} \|Lu(x, t)\|^2 dx dt < \int_0^1 \int_{\Omega} \|Lv(x, t)\|^2 dx dt$ contradicts the assumption that $v(x, t)$ is the minimizer of the energy E . □

The exact matching problem can be generalized to the *inexact matching problem*. In the inexact matching problem, we do not require that the points exactly match. Instead, we seek a compromise between the closeness of the matching points and the deformation of space. We minimize

$$\int_0^1 \int_{\Omega} \|Lv(x, t)\|^2 dx dt + \lambda \sum_{i=1}^n \|q_i - \phi(p_i, 1)\|^2, \quad (1.26)$$

which can be similarly solved.

3 Diffeomorphic Point Shape Matching

In the diffeomorphic point matching problem, the points are samples from the shape and we have a point representation of the shape. When we have two such shapes represented by points, usually the cardinality of the points in the two shape point-sets are different and there is no point-wise correspondence. We want to find the correspondence between the two shapes. The approach we take is clustering. The two point shapes are clustered simultaneously and we assume there is a one-to-one correspondence between the clusters. The correspondences between the two sets of clusters are, unfortunately, also unknown. We put the correspondence and the diffeomorphism together and by minimizing an objective function which has both the clustering energy and the diffeomorphic deformation energy, we are able to find the clustering, the correspondence between cluster centers and the diffeomorphism in space simultaneously. The objective function is

$$\begin{aligned}
 & E(M^x, M^y, r, s, v, \phi) \\
 = & \sum_{i=1}^{N_1} \sum_{k=1}^N M_{ik}^x \|x_i - r_k\|^2 + \sum_{j=1}^{N_2} \sum_{k=1}^N M_{jk}^y \|y_j - s_k\|^2 \quad (1.27) \\
 & + \sum_{k=1}^N \|s_k - \phi(r_k, 1)\|^2 + \lambda \int_0^1 \int_{\Omega} \|Lv(x, t)\|^2 dx dt.
 \end{aligned}$$

In the above objective function, the M^x and M^y are the cluster membership matrices, which satisfy $M_{ik}^x \in [0, 1]$, $\forall ik$ and $M_{jk}^y \in [0, 1]$, $\forall jk$ and $\sum_{k=1}^N M_{ik}^x = 1$, $\sum_{k=1}^N M_{jk}^y = 1$. The matrix entry M_{ik}^x is the membership of data point x_i in cluster k whose center is at location r_k . The matrix entry M_{jk}^y is the membership of data point y_j in cluster k whose center is at position s_k . Point-set X has N_1 points, Y has N_2 points and the number of shared cluster centers is N .

The diffeomorphic deformation energy in Ω is induced by the landmark displacements from r to s , where $x \in \Omega$ and $\phi(x, t)$ is the one parameter diffeomorphism: $\Omega \rightarrow \Omega$. Since the original point-sets differ in point count and are unlabeled, we cannot immediately use the diffeomorphism objective functions as in [14] or [3] respectively. Instead, the two point-sets are clustered and the landmark diffeomorphism objective is used between two sets of cluster centers r and s whose indices are always in correspondence. The diffeomorphism $\phi(x, t)$ is generated by the velocity field $v(x, t)$. $\phi(x, t)$ and $v(x, t)$ together satisfy the transport equation $\frac{d\phi(x, t)}{dt} = v(\phi(x, t), t)$ and the initial condition $\forall x, \phi(x, 0) = x$ holds. This is in the inexact matching form and the displacement term $\sum_{k=1}^N \|s_k - \phi(r_k, 1)\|^2$ plays an important role here as the bridge between the two systems. This is also the reason why we prefer the deformation energy in this form because the coupling of the

two sets of clusters appear naturally through the inexact matching term and we don't have to introduce external coupling terms as in [12]. Another advantage of this approach is that in this dynamic system described by the diffeomorphic group $\phi(x, t)$, the landmarks trace a trajectory exactly on the flow lines dictated by the field $v(x, t)$. Also, the feedback coupling is no longer needed as in the previous approach because with this deformation energy described above, due to the above theorem, if $\phi(x, t)$ is the minimizer of this energy, then $\phi^{-1}(x, t)$ is the inverse mapping which also minimizes the same energy.

We are now ready to give an algorithm that simultaneously finds the cluster centers, the correspondence and the diffeomorphism.

The joint clustering and diffeomorphism estimation algorithm has two components: i) diffeomorphism estimation and ii) clustering. For the diffeomorphism estimation, we expand the velocity field in term of the kernel K of the L operator

$$v(x, t) = \sum_{k=1}^N \alpha_k(t) K(x, \phi_k(t)) \quad (1.28)$$

where $\phi_k(t)$ is notational shorthand for $\phi(r_k, t)$ and we also take into consideration the affine part of the mapping when we use thin-plate spline kernel with matrix entry $K_{ij} = r_{ij}^2 \log r_{ij}$ and $r_{ij} = \|x_i - x_j\|$. After discretizing in time t , the objective in 1.27 is expressed as

$$\begin{aligned} E = & \sum_{i=1}^{N_1} \sum_{k=1}^N M_{ik}^x \|x_i - r_k\|^2 + \sum_{j=1}^{N_2} \sum_{k=1}^N M_{jk}^y \|y_j - s_k\|^2 \quad (1.29) \\ & + \sum_{k=1}^N \|s_k - r_k - \sum_{l=1}^N \sum_{t=0}^S [P(t)d_l(t) + \alpha_l(t)K(\phi_k(t), \phi_l(t))]\|^2 \\ & + \lambda \sum_{k=1}^N \sum_{l=1}^N \sum_{t=0}^S \langle \alpha_k(t), \alpha_l(t) \rangle K(\phi_k(t), \phi_l(t)) \end{aligned}$$

where

$$P(t) = \begin{pmatrix} 1 & \phi_1^1(t) & \phi_1^2(t) \\ \cdot & \cdot & \cdot \\ \cdot & \cdot & \cdot \\ \cdot & \cdot & \cdot \\ 1 & \phi_N^1(t) & \phi_N^2(t) \end{pmatrix} \quad (1.30)$$

and d is the affine parameter matrix. We then perform a QR decomposition on P ,

$$P(t) = (Q_1(t) : Q_2(t)) \begin{pmatrix} R(t) \\ 0 \end{pmatrix}. \quad (1.31)$$

We iteratively solve for $\alpha_k(t)$ and $\phi_k(t)$ using an alternating algorithm. When $\phi_k(t)$ is held fixed, we use the following approximation to solve for $\alpha_k(t)$. The solutions are

$$d(t) = R^{-1}(t) [Q_1(t)\phi(t+1) - Q_1(t)K(\phi(t))Q_2(t)\gamma(t)] \quad (1.32)$$

$$\alpha(t) = Q_2(t)\gamma(t) \quad (1.33)$$

where $K(\phi(t))$ denotes the thin-plate spline kernel *matrix* evaluated at $\phi(t) \stackrel{\text{def}}{=} \{\phi(r_k, t) | k = 1, \dots, N\}$ and

$$\gamma(t) = (Q_2^T(t)K(\phi(t))Q_2(t) + \lambda)^{-1}Q_2^T(t)\phi(t+1). \quad (1.34)$$

When $\alpha_k(t)$ is held fixed, we use gradient descent to solve for $\phi_k(t)$:

$$\frac{\partial E}{\partial \phi_k(t)} = 2 \sum_{l=1}^N \langle \alpha_k(t), \alpha_l(t) - 2W_l \rangle \nabla_1 K(\phi_k(t), \phi_l(t)) \quad (1.35)$$

where $W_l = s_l - r_l - \sum_{m=1}^N \int_0^1 \alpha_m(t) K(\phi_m(t), \phi_l(t)) dt$.

The clustering of the two point-sets is handled by a deterministic annealing EM algorithm which iteratively estimates the cluster memberships M^x and M^y and the cluster centers \mathbf{r} and \mathbf{s} . The update of the memberships is the very standard E-step of the EM algorithm [6] and is performed as shown below.

$$M_{ik}^x = \frac{\exp(-\beta \|x_i - r_k\|^2)}{\sum_{l=1}^N \exp(-\beta \|x_i - r_l\|^2)}, \forall ik \text{ and} \quad (1.36)$$

$$M_{jk}^y = \frac{\exp(-\beta \|y_j - s_k\|^2)}{\sum_{l=1}^N \exp(-\beta \|y_j - s_l\|^2)}, \forall jk \quad (1.37)$$

where $\beta = \frac{1}{T}$ is the inverse temperature. The cluster center update is the M-step of the EM algorithm. This step is not the typical M-step. We use a closed-form solution for the cluster centers which is an approximation. From the clustering standpoint, we assume that the change in the diffeomorphism at each iteration is *sufficiently small so that it can be neglected*. After making this approximation, we get

$$r_k = \frac{\sum_{i=1}^{N_1} M_{ik}^x x_k + s_k - \sum_{l=1}^N \int_0^1 \alpha_l(t) K(\phi_l(t), \phi_k(t)) dt}{1 + \sum_{i=1}^{N_1} M_{ik}^x}, \quad (1.38)$$

$$s_k = \frac{\sum_{j=1}^{N_2} M_{jk}^y y_j + \phi(r_k, 1)}{1 + \sum_{j=1}^{N_2} M_{jk}^y}, \forall k. \quad (1.39)$$

In the clustering and diffeomorphic estimation steps, we let λ vary proportionally with the temperature. This controls the rigidity of the mapping, starting from an almost rigid mapping while we obtain good correspondence and gradually softens so that good clustering is achieved. In this way both clustering and diffeomorphism are obtained simultaneously at convergence.

The overall algorithm is described below.

- **Initialization:** Initial temperature
 $T = 0.5(\max_i \|x_i - x_c\|^2 + \max_j \|y_j - y_c\|^2)$ where x_c and y_c are the centroids of X and Y respectively.
- **Begin A:** While $T > T_{\text{final}}$
 - **Step 1:** Clustering
Update memberships according to (1.36), (1.37).
Update cluster centers according to (1.38), (1.39).
 - **Step 2:** Diffeomorphism
Update (ϕ, v) by minimizing

$$E_{\text{diff}}(\phi, v) = \sum_{k=1}^N \|s_k - \phi(r_k, 1)\|^2 + \lambda T \int_0^1 \int_{\Omega} \|Lv(x, t)\|^2 dx dt$$

according to (1.32)(1.33) and (1.35).

- **Step 3:** Annealing. $T \leftarrow \gamma T$ where $\gamma < 1$.

- **End**

Next we show the experimental results applying the algorithm to nine sets of 2D corpus callosum slices. The feature points were extracted with the help of a neuroanatomical expert. Figure 3 shows the nine corpus callosum 2D images, labeled CC1 through CC9. In our experiments, we first did the simultaneous clustering and matching with the corpus callosum point sets CC5 and CC9. The clustering of the two point sets is shown in Figure 4. There are 68 cluster centers. The circles represent the centers and the dots are the data points. The two sets of cluster centers induce the diffeomorphic mapping of the 2D space. The warping of the 2D grid under this diffeomorphism is shown in Figure 5. Using this diffeomorphism, we calculated the after-image of original data points and compared them with the target data points. Due to the large number of cluster centers, the cluster centers nearly coincide with the original data points and the warping of the original data points is not shown in the figure. The correspondences (at the cluster level) are shown in Figure 6. The algorithm allows us to simultaneously obtain the diffeomorphism and the correspondence.

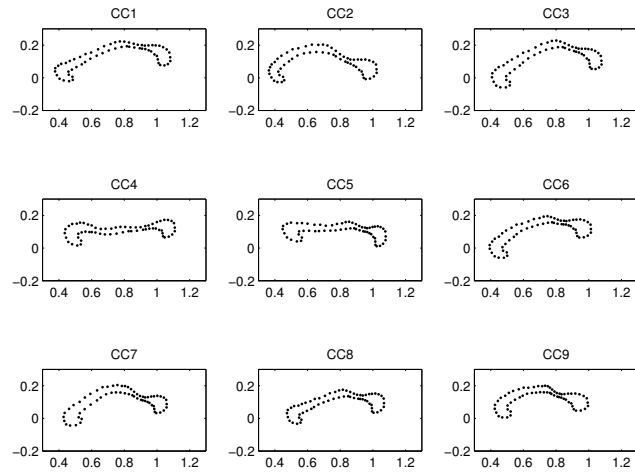


FIGURE 3. Point sets of nine corpus callosum images.

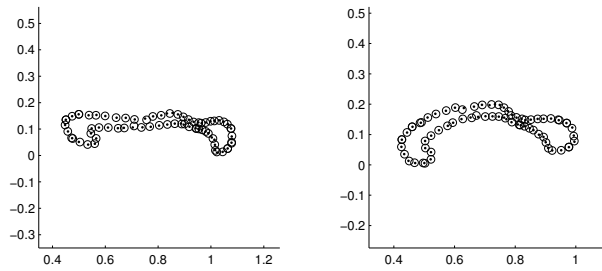


FIGURE 4. Clustering of the two point sets.

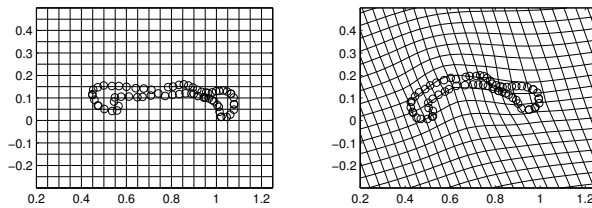


FIGURE 5. Diffeomorphic mapping of the space.

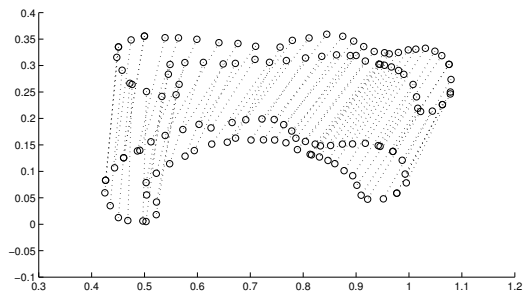


FIGURE 6. Matching between the two point sets.

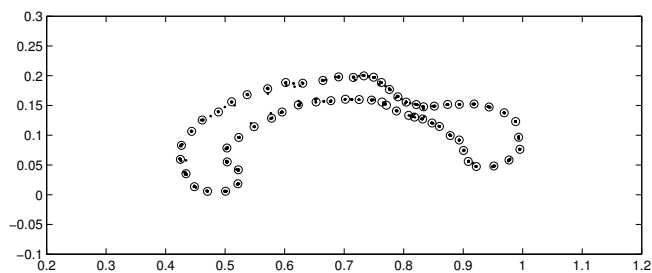


FIGURE 7. Overlay of the after-images of eight point sets with the ninth set.

4 Discussion

There are other approaches to the diffeomorphic point matching problem which we have not considered here. One indirect approach is to use distance transforms to convert the point matching problem into an image matching problem. There are as yet no theoretical and/or experimental comparisons between distance transforms-based diffeomorphisms and our approach. Also, there are other approaches to diffeomorphic landmark matching [3, 12]. While we have only provided results for 2D diffeomorphic point matching, the theoretical formulation presented here extends to 3D. Finally, the joint clustering and matching formulation is not the only approach that in principle can marry diffeomorphisms and correspondence [5]. However, it appears to be the simplest formulation that does not require us to establish point correspondences via estimation of permutations.

5 REFERENCES

- [1] F.L. Bookstein. Principal Warps: Thin-plate Splines and the Decomposition of Deformations. *IEEE Trans. Patt. Anal. Mach. Intell.*, 11(6):567–585, June 1989.
- [2] F.L. Bookstein. *Morphometric Tools for Landmark Data: Geometry and Biology*. Cambridge University Press, 1991.
- [3] V. Camion and L. Younes. Geodesic Interpolating Splines. In *Energy Minimization Methods for Computer Vision and Pattern Recognition*, pages 513–527. Springer, New York, 2001.
- [4] G. Christensen. Consistent Linear-elastic Transformations for Image Matching. In *Proceedings of Information Processing in Medical Imaging—IPMI 99*, pages 224–237. Springer-Verlag, 1999.
- [5] H. Chui and A. Rangarajan. A New Point Matching Algorithm for Non-rigid Registration. *Computer Vision and Image Understanding*, 89:114–141, 2003.
- [6] H. Chui, L. Win, J. Duncan, R. Schultz, and A. Rangarajan. A Unified Non-rigid Feature Registration Method for Brain Mapping. *Medical Image Analysis*, 7:112–130, 2003.
- [7] T. Cootes, C. Taylor, D. Cooper, and J. Graham. Active Shape Models: Their Training and Application. *Computer Vision and Image Understanding*, 61(1):38–59, 1995.
- [8] J. Duchon. *Splines Minimizing Rotation-invariant Semi-norms in Sobolev Spaces, in Constructive Theory of Functions of Several Variables*, pages 85–100. Springer-Verlag, 1977.
- [9] P. Dupuis, U. Grenander, and M.I. Miller. Variational Problems on Flows of Diffeomorphisms for Image Matching. *Quarterly of Applied Math.*, 56:587–600, 1998.
- [10] J. Feldmar and N Ayache. Rigid, Affine and Locally Affine Registration of Free-Form Surfaces. *Intl. J. Computer Vision*, 18(2):99–119, May 1996.
- [11] F. Girosi, M. Jones, and T. Poggio. Regularization Theory and Neural Network Architectures. *Neural Computation*, 7:219–269, 1995.
- [12] H. Guo, A. Rangarajan, S. Joshi, and L. Younes. Non-rigid Registration of Shapes via Diffeomorphic Point Matching. *ISBI 2004*, 2004.
- [13] H.J. Johnson and G.E. Christensen. Consistent Landmark and Intensity-Based Image Registration. *IEEE Transactions on Medical Imaging*, 21:450–469, 2002.

- [14] S. Joshi and M. Miller. Landmark Matching via Large Deformation Diffeomorphisms. *IEEE Trans. Image Processing*, 9:1357–1370, 2000.
- [15] G. Kimeldorf and G. Wahba. Some Results on Tchebycheffian Spline Functions. *Journal of Mathematical Analysis and Applications*, 33(1):82–95, 1971.
- [16] M. Miller, S. Joshi, and G. Christensen. *Brain Warping*, pages 131–155. Academic Press, 1998.
- [17] G. Wahba. *Spline Models for Observational Data*. SIAM, Philadelphia, PA, 1990.